



# Electrophoretic deposition of silica–hyaluronic acid and titania–hyaluronic acid nanocomposites

R. Ma, I. Zhitomirsky\*

Department of Materials Science and Engineering, McMaster University, 1280 Main Street West, Hamilton, Ontario, Canada, L8S 4L7

## ARTICLE INFO

### Article history:

Received 4 June 2010

Received in revised form

15 September 2010

Accepted 24 October 2010

Available online 3 November 2010

### Keywords:

Hyaluronic acid

Silica

Titania

Electrophoretic deposition

Nanocomposite

Film

## ABSTRACT

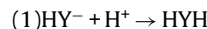
Thin films of hyaluronic acid were prepared by anodic electrophoretic deposition (EPD) and the deposition kinetics was studied using quartz crystal microbalance. EPD method has been developed for the fabrication of new ceramic–biopolymer nanocomposites containing silica and titania nanoparticles in the matrix of hyaluronic acid. The deposit thickness was varied in the range of 0–10 μm. The composition of the deposits can be varied by the variation of silica and titania concentration in the suspensions. The deposits were studied by thermogravimetric analysis, differential thermal analysis, Fourier transform infrared spectroscopy, X-ray diffraction analysis, and scanning electron microscopy. The method offers the advantages of room temperature processing of nanocomposite materials for biomedical applications.

© 2010 Elsevier B.V. All rights reserved.

## 1. Introduction

Hyaluronic acid (HYH) is a natural biopolymer, which is present in high concentrations in skin, joints and cornea. It is widely used as a coating for the surface modification of various biomaterials for prosthetic cartilage, vascular grafts, guided nerve regeneration and drug delivery [1,2]. HYH is non-immunogenic, non-adhesive, bioactive material that has been associated with several cellular processes, including angiogenesis and the regulation of inflammation [3]. It was shown that HYH binds to cells and effectively promotes new bone formation [4]. Significant interest has been generated in the fabrication of organic–inorganic nanocomposites containing HYH for applications in biomedical implants. Such composites have attracted substantial attention because of the possibility of combining the functional properties of HYH and inorganic components [5]. The combination of polymeric and inorganic phases is a common feature of various natural materials, including bone. The organic–inorganic nanocomposites containing silica and titania are attractive materials for the fabrication of osseointegrative implants, because nanostructured silica and titania promote the spontaneous formation of bone-like apatites in physiological solutions.

The goal of this investigation was the fabrication of HYH–silica and HYH–titania nanocomposites by electrophoretic deposition (EPD). Electrophoresis is of high importance in biotechnology for manipulation of biological materials, e.g. biopolymers, bioceramics, proteins, enzymes and cells. EPD [6] is a promising method for fabricating composite films containing biopolymers and inorganic nanoparticles. Recently HYH films were prepared by EPD from sodium hyaluronate (HYNa) solutions [7]. The deposition mechanism is based on the electrophoretic motion of the anionic hyaluronate macromolecules  $\text{HY}^-$  toward the anode and the formation of HYH films in the low pH region at the anode surface:



These results pave the way for the fabrication of composite films containing inorganic nanoparticles in the HYH matrix. The experimental data presented below indicated that  $\text{HY}^-$  provided efficient dispersion and charging of silica and titania particles in the suspensions. Nanocomposite films of controlled mass and composition were obtained by electrophoretic co-deposition of the inorganic particles and HYH.

## 2. Experimental procedures

Sodium hyaluronate (HYNa) (Alfa Aesar), silica (amorphous, average particle size 7 nm, Aldrich) and titania (anatase, average particle size 25 nm, Aldrich) were used as starting materials. The electrodeposition cell included a substrate and Pt counterelectrode. The distance between the substrate and counterelectrode was 15 mm. Deposition was performed from HYNa solutions in a mixed ethanol–water (30% water) solvent containing silica or titania at the deposition voltage of 4–20 V during 1–10 min. The deposition of thin HYH films was investigated in-situ using a quartz

\* Corresponding author. Tel.: +1 905 525 9140; fax: +1 905 528 9295.  
E-mail address: [zhitom@mcmaster.ca](mailto:zhitom@mcmaster.ca) (I. Zhitomirsky).

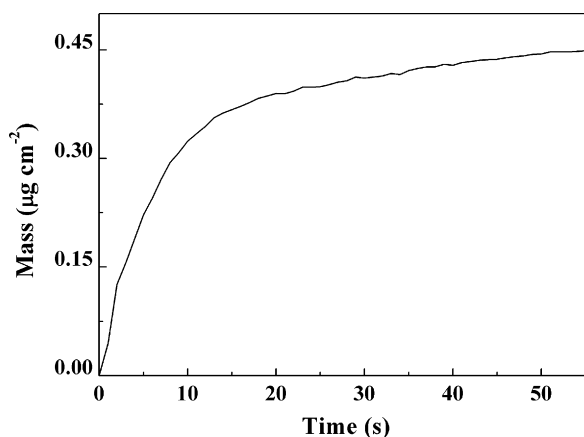


Fig. 1. Deposit mass, measured using QCM, as a function of the deposition time for the  $0.2 \text{ g L}^{-1}$  HYN a solution at a deposition voltage of 4 V.

crystal microbalance (QCM 922, Princeton Applied Research, frequency 9 MHz) controlled by a computer. The area of the gold coated quartz electrode was  $0.2 \text{ cm}^2$ . The composite silica–HYH and titania–HYH films were obtained on Pt, graphite and 304 stainless steel ( $50 \text{ mm} \times 50 \text{ mm} \times 0.1 \text{ mm}$ ) substrates and dried in air for 48 h. Deposition yield was studied after drying of the deposits formed on the stainless steel substrates. The deposits were removed from the Pt substrates for thermogravimetric analysis (TGA), differential thermal analysis (DTA) and Fourier transform infrared spectroscopy (FTIR). TGA and DTA studies were carried out in air at a heating rate of  $5^\circ \text{ C min}^{-1}$  using thermoanalyzer (Netzsch STA-409). FTIR investigations were performed on Bio-Rad FTS-40 instrument. The cross sections (fractures) of the films deposited on graphite substrates were investigated using a JEOL JSM-7000F scanning electron microscope (SEM). The X-ray diffraction (XRD) studies were performed using a powder diffractometer (Nicolet I2, monochromatized  $\text{CuK}\alpha$  radiation) at a scanning speed of  $0.5^\circ \text{ min}^{-1}$ .

### 3. Results and discussion

The EPD yield was investigated using suspensions containing  $0\text{--}1 \text{ g L}^{-1}$  HYN a and  $0\text{--}1.2 \text{ g L}^{-1}$  silica or titania. Fig. 1 shows deposit mass, measured using QCM, as a function of deposition time for pure HYH deposit. The slope of the curve (Fig. 1) decreased with increasing deposition time and indicated the decrease in the deposition rate. The decrease in the deposition rate with time can be attributed to the decrease in voltage drop in the suspension, which resulted from the increasing voltage drop in the insulating HYH layer formed at the anodic substrate. The increase in the deposit mass with time indicated the formation of HYH films of differ-

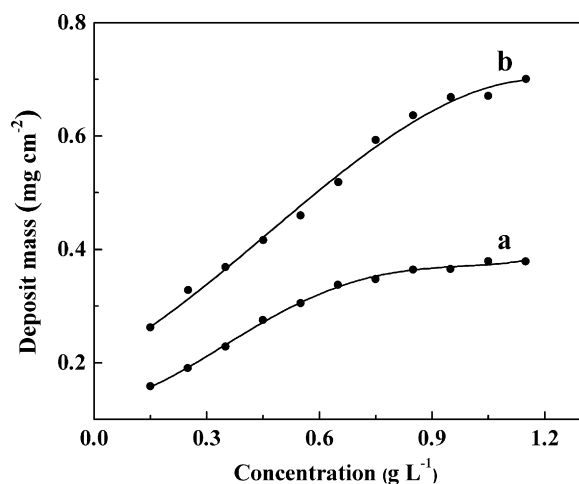


Fig. 2. Deposit mass versus concentration of (a) silica and (b) titania in suspensions, containing  $0.5 \text{ g L}^{-1}$  HYN a, for the deposits prepared at a constant voltage of 20 V and deposition time of 5 min.

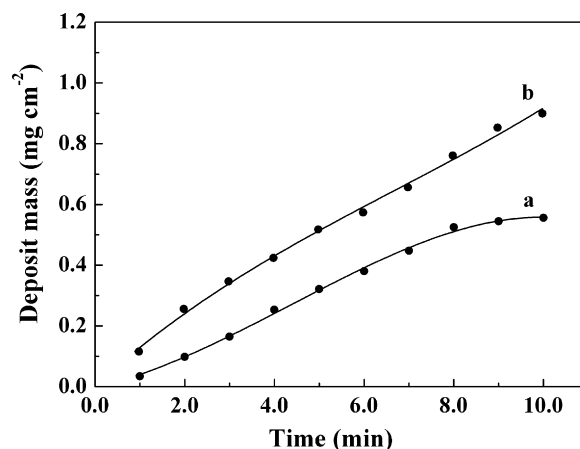


Fig. 3. Deposit mass versus deposition time for the deposits prepared from (a)  $0.65 \text{ g L}^{-1}$  silica and (b)  $0.65 \text{ g L}^{-1}$  titania suspensions, containing  $0.5 \text{ g L}^{-1}$  HYN a at a constant voltage of 20 V.

ent thickness from HYN a solutions. However no deposition was observed from pure silica or titania suspensions without HYN a. Sedimentation experiments showed, that the addition of HYN a to the suspensions of silica and titania resulted in improved suspension stability. Moreover, anodic deposits were obtained from silica and titania suspensions containing HYN a. Therefore, silica and titania particles were negatively charged in the HYN a solutions. It is suggested that particle charge and improved suspension stability are attributed to the adsorption of anionic  $\text{HY}^-$  species on the surfaces of silica and titania particles.

Fig. 2 shows deposit mass as a function of silica and titania concentration in the suspensions containing  $0.5 \text{ g L}^{-1}$  HYN a. The deposited films were mechanically stable and adhered well to the substrates. The increase in particle concentration in the suspensions resulted in increasing deposition yield. The higher deposition yield can be attributed to higher concentration of the particles in the deposits. It is suggested that the co-deposition of  $\text{HY}^-$  species and ceramic particles containing adsorbed  $\text{HY}^-$  resulted in the formation of composite silica–HYH and titania–HYH films. Moreover, the results indicated that film composition can be varied by the variation of silica or titania concentration in the suspensions. The

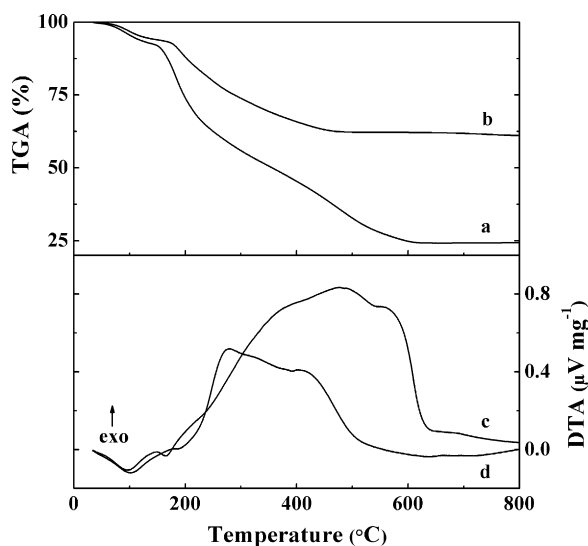
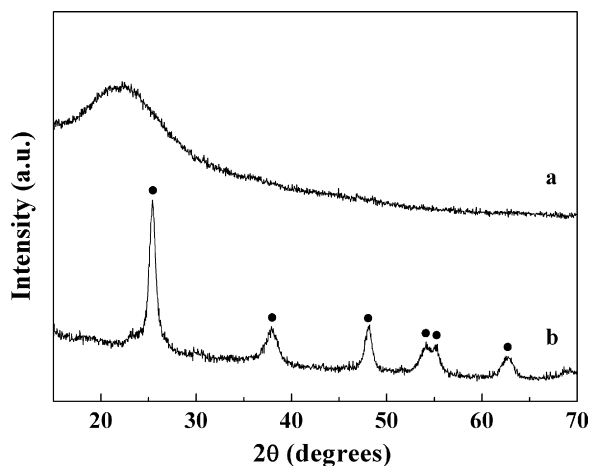


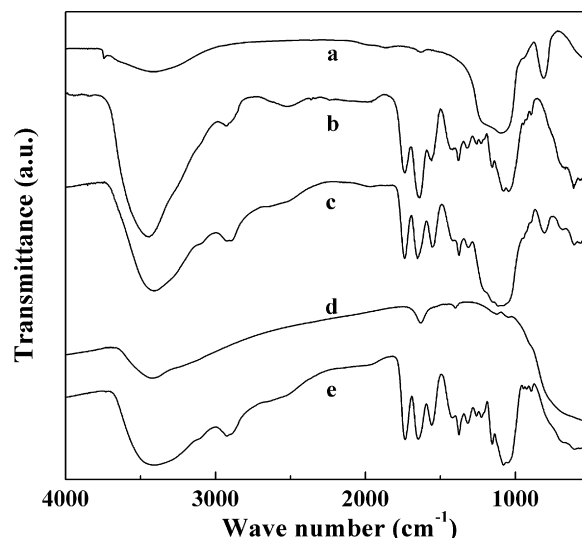
Fig. 4. (a and b) TGA and (c and d) DTA data for deposits prepared from (a and c)  $0.15 \text{ g L}^{-1}$  silica and (b and d)  $0.15 \text{ g L}^{-1}$  titania suspensions containing  $0.5 \text{ g L}^{-1}$  HYN a at a constant voltage of 20 V.



**Fig. 5.** X-ray diffraction patterns for deposits prepared from (a)  $0.65 \text{ g L}^{-1}$  silica and (b)  $0.65 \text{ g L}^{-1}$  titania suspensions, containing  $0.5 \text{ g L}^{-1}$  HYN a at a constant voltage of 20 V (● - anatase, JCPDS file 21-1272).

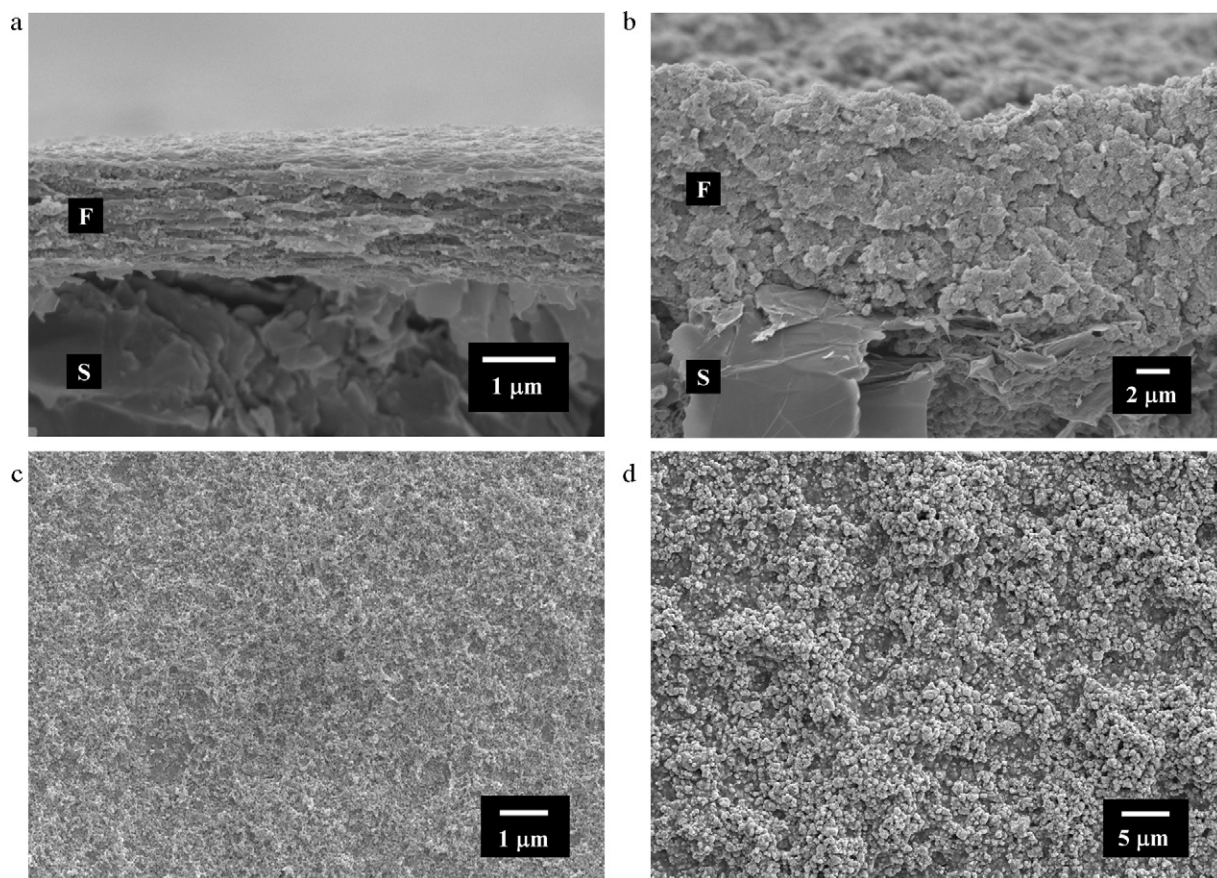
deposit mass increased with increasing deposition time, as shown in Fig. 3. Therefore, the amount of the deposited material can be varied.

Fig. 4 shows typical TGA and DTA data for the deposits. The observed mass loss in the TGA data below  $200^\circ\text{C}$  and corresponding broad endotherms in the DTA data can be attributed to dehydration. The mass loss at higher temperatures (Fig. 4a and b) and corresponding broad exotherms (Fig. 4c and d) are related to burning out of HYH. The deposits containing silica and titania showed mass loss



**Fig. 6.** FTIR spectra for (a) as-received silica, (b) deposit prepared from  $0.5 \text{ g L}^{-1}$  HYN a solution (c) deposit prepared from  $0.65 \text{ g L}^{-1}$  silica suspension containing  $0.5 \text{ g L}^{-1}$  HYN a, (d) as-received titania, and (e) deposit prepared from  $0.65 \text{ g L}^{-1}$  titania suspension, containing  $0.5 \text{ g L}^{-1}$  HYN a, deposits were obtained at a constant voltage of 20 V.

below  $600$ , and  $500^\circ\text{C}$ , respectively. The sample mass was nearly constant at higher temperatures. The total mass loss at  $800^\circ\text{C}$  was found to be 76 and 39 mass% for the deposits prepared from the suspensions containing  $0.15 \text{ g L}^{-1}$  silica and  $0.15 \text{ g L}^{-1}$  titania, respectively. The results presented in Fig. 4 indicated the forma-



**Fig. 7.** SEM images of (a,b) cross sections (fractures) and (c and d) surfaces of deposits prepared from (a and c)  $0.65 \text{ g L}^{-1}$  silica and (b and d)  $0.65 \text{ g L}^{-1}$  titania suspensions, containing  $0.5 \text{ g L}^{-1}$  HYN a on graphite substrates (F - film, S - substrate) at a constant voltage of 20 V.

tion of composite films, containing 24 mass% of silica and 61 mass% of titania in the HYH matrix. The TGA and DTA data showed that the burning out of HYH was observed at higher temperatures for the composite containing silica, compared to the composite containing titania (Fig. 4). It is known that thermal degradation of composite nanomaterials is influenced by surface complexation of organic and inorganic components [8]. Such surface complexation can be attributed to the interaction of  $\text{COO}^-$  and  $\text{NH}$  groups of hyaluronate with Si and Ti atoms at the particle surface. It is suggested that smaller particle size and higher surface area of the silica particles resulted in enhanced surface complexation of the organic and inorganic components, which, in turn, resulted in different thermal behaviour of the composite films. The results of TGA and DTA studies are in a good agreement with XRD data, which indicated the formation of composite films. The XRD studies of silica–HYH deposits revealed a broad amorphous halo at  $2\theta \sim 23^\circ$  (Fig. 5), the XRD patterns of titania–HYH deposits (Fig. 5) showed peaks of anatase in agreement with the data provided by the powder manufacturer.

The results of FTIR investigations are shown in Fig. 6. The FTIR spectrum of as-received silica (Fig. 6a) showed the typical broad band in the wave number region  $1000\text{--}1150\text{ cm}^{-1}$  and at a band at  $808\text{ cm}^{-1}$  attributed to Si–O–Si stretching [9,10]. The band at  $1739\text{ cm}^{-1}$  in the spectrum of the deposit (Fig. 6b) prepared from the HYNa solution is related to the stretching of the protonated carboxylic group of HYH. The amide I and amide II bands of HYH [11] were observed at  $1643$  and  $1560\text{ cm}^{-1}$ , respectively. The FTIR spectrum of the deposit prepared from the silica suspensions containing HYNa (Fig. 6c) showed similar bands. The FTIR spectrum of as-received titania showed a band at  $1631\text{ cm}^{-1}$ , attributed to bending vibration of adsorbed water [12] and the broad absorption below  $800\text{ cm}^{-1}$  is attributed to the characteristic adsorptions of titania [12,13]. The FTIR spectrum of the deposit prepared from titania suspension containing HYNa showed absorptions attributed to the stretching of the protonated carboxylic group of HYH, amide I, amide II and other characteristic adsorptions of titania. Therefore, the FTIR data showed the formation of composite silica–HYH and titania–HYH films.

The composite deposits were studied by SEM. Fig. 7 shows typical images of the cross sections and surfaces of the composite deposits. The thickness of the deposits was varied in the range of  $0\text{--}10\text{ }\mu\text{m}$  by the variation of the deposition time. The deposits were relatively dense, crack free and contained silica and titania particles in the HYH matrix. SEM observations showed that the size of the particles in the deposits is in a good agreement with the data

provided by powder manufacturer. The use of HYH with good film forming and binding properties enabled the formation of nanocomposite coatings. It should be noted that the fabrication of ceramic coatings by EPD presents difficulties, attributed to sintering. The sintering of ceramic deposits on metallic substrates can result in cracking, attributed to drying shrinkage, changes in deposit microstructure, related to grain growth, and changes in composition, related to diffusion and thermal degradation of the substrates at elevated temperatures. The method developed in this work offers the advantages of room temperature processing of composite materials. In this approach, the problems related to deposit sintering can be avoided. It is suggested that the nanocomposite materials, combining functional properties of HYH, nanostructured silica and titania, can be utilized for biomedical applications.

#### 4. Conclusions

EPD method has been developed for the co-deposition of HYH, silica and titania. The results of the deposition yield measurements, TGA, DTA, XRD, FTIR and SEM studies showed the formation of silica–HYH and titania–HYH nanocomposites. The deposit composition can be varied by the variation of the concentration of ceramic particles in the suspensions. The deposit thickness can be varied in the range of  $0\text{--}10\text{ }\mu\text{m}$  by the variation of the deposition time. The method offers the advantages of room temperature processing for the fabrication of organic–inorganic nanocomposites for biomedical applications.

#### References

- [1] M. Mason, K.P. Vercruyse, K.R. Kirker, R. Frisch, D.M. Marecak, G.D. Prestwich, W.G. Pitt, *Biomaterials* 21 (2000) 31–36.
- [2] Y. Li, T. Nagira, T. Tsuchiya, *Biomaterials* 27 (2006) 1437–1443.
- [3] J.B. Leach, C.E. Schmidt, *Biomaterials* 26 (2005) 125–135.
- [4] M. Yoshikawa, N. Tsuji, T. Toda, H. Ohgushi, *Materials Science and Engineering C* 27 (2007) 220–226.
- [5] G. Khachatryan, K. Khachatryan, L. Stobinski, P. Tomasik, M. Fiedorowicz, H.M. Lin, *Journal of Alloys and Compounds* 481 (2009) 402–406.
- [6] I. Zhitomirsky, *Advances in Colloid and Interface Science* 97 (2002) 277–315.
- [7] F. Sun, I. Zhitomirsky, *Surface Engineering* 25 (2009) 621–627.
- [8] Y. Li, K. Wu, I. Zhitomirsky, *Physicochemical and Engineering Aspects* 356 (2010) 63–70.
- [9] J. Vega-Baudrit, V. Navarro-Bañón, P. Vázquez, J.M. Martín-Martínez, *International Journal of Adhesion and Adhesives* 26 (2006) 378–387.
- [10] V.M. Gun'ko, et al., *Journal of Colloid and Interface Science* 289 (2005) 427–445.
- [11] A.L.R. Mercê, L.C. Marques Carrera, L.K. Santos Romanholi, M.Á. Lobo Recio, *Journal of Inorganic Biochemistry* 89 (2002) 212–218.
- [12] K. Porkodi, S.D. Arokiamary, *Materials Characterization* 58 (2007) 495–503.
- [13] E. Sánchez, T. López, R. Gómez, Bokhimi, A. Morales, O. Novaro, *Journal of Solid State Chemistry* 122 (1996) 309–314.